



## **Progress Report on: Investigation of the Physical-chemistry of Carbonated Water Flooding**

Prepared by: K-H Wolf, Delft University of Technology  
C.Hofstee, TNO  
A. Peksa, Delft University of Technology

Reviewed by: K-H Wolf, Delft University of Technology

Approved by: J.Brouwer  
(CATO-2 Director)



## 1 Executive Summary (restricted)

WP3.5.3:

*D12: Investigation of the physical-chemistry of Carbonated Water Flooding (CO<sub>2</sub>) EOR&EGR*

*CO<sub>2</sub>-EGR:*

TNO concentrates on EGR field-activities, spending time on all kind of questions coming from various sources surrounding the P18 storage compartment, i.e. cooperation with work-packages within the SP's 2 and 3, Capture and Transportation, C. Hofstee models various reservoirs on their transport/storage behaviour. This work involves various EGR scenario's for the P18-2, 18-4 and K12B fields. The work is confidential. Appendix 2 gives a summary of the activities.

*CO<sub>2</sub>-EOR:*

- A.Peksa performs theoretical and experimental work under supervision of K-H. Wolf. and Prof. dr. Pacelli Zitha. Preliminary results are presented in appendix 3.
- Again, the section from the work done in Task 3.5.3, i.e. CO<sub>2</sub>-EOR activities, has been merged with WP3.2 and reported in WP3.2, i.e. wettability behaviour.
- A part of the work on dielectric behaviour of the water-oil-sandstone system is in cooperation with WP3.8 and reported by R. Ghose, D. Draganov and A. Kirichek

For WP3.5.3, we continue as planned, following the CO<sub>2</sub>-EOR/EGR activities as described in the deliverables (3.5.3.D12). Plans for 2013 for the PhD: The goal of future study is to determine the surface behaviour of the silicon oxide and Bentheimer sandstone. In addition obtain the answer for following questions:

- How CO<sub>2</sub> dissolved in water (aqueous H<sub>2</sub>CO<sub>3</sub>) altered wettability (if it goes towards more water wet or oil wet – at temperatures ranging from 30 to 40 °C and at different pressures)
- How do CO<sub>2</sub> in water change the charges of rock /brine (rock/distilled water; oil/ brine) interface and the thickness of double layer? Additionally, it is planned to finalize the on-going studies as described in Deliverable D3.05.12

## Distribution List

(this section shows the initial distribution list)

External	copies	Internal	Copies
	2	TNO	1
		TUD	1

## Document Change Record

(this section shows the historical versions, with a short description of the updates)

Version	Nr of pages	Short description of change	Pages
3.5.2-D05	1 - 23	On-going work on field development of the doublets, associated petrophysical results and modelling work	6 - 23

## Table of Content

<b>1</b>	<b>Executive Summary (restricted)</b> .....	<b>2</b>
<b>2</b>	<b>Applicable/Reference documents and Abbreviations</b> .....	<b>4</b>
2.1	Applicable Documents .....	4
2.2	Reference Documents .....	4
2.3	Abbreviations .....	4
<b>3</b>	<b>Various EGR scenario's for the P18-2 and K12B fields.(confidential).....</b>	<b>5</b>
<b>4</b>	<b>CO<sub>2</sub>-EOR activities and results over 2012</b> .....	<b>6</b>

## 2 Applicable/Reference documents and Abbreviations

### 2.1 Applicable Documents

(Applicable Documents, including their version, are the “legal” basis to the work performed)

	<b>Title</b>	<b>Doc nr</b>	<b>Version</b>
AD-01d	Toezegging CATO-2b	FES10036GXDU	2010.08.05
AD-01f	Besluit wijziging project CATO2b	FES1003AQ1FU	2010.09.21
AD-02a	Consortium Agreement	CATO-2-CA	2009.09.07
AD-02b	CATO-2 Consortium Agreement	CATO-2-CA	2010.09.09
AD-03g	Program Plan 2013	CATO2-WP0.A-D03	2013.04.01

### 2.2 Reference Documents

(Reference Documents are referred to in the document)

	<b>Title</b>	<b>Doc no</b>	<b>No</b>

### Invited talks, presentations and abstracts

### 2.3 Abbreviations

(this refers to abbreviations used in this document)


### 3 Various EGR scenario's for the P18-2 and K12B fields.(confidential)

#### K12B

In 2012, a new attempt was made to update the history match of the K12B compartment 3 using all available data and interpretations. The main objective was to get a more realistic geological model, by reducing or eliminating the multipliers used for the earlier history match. This work was conducted by Gas de France Suez (Paris) together with TNO. The updated reservoir model was subsequently used to predict the impact of converting a current producer into an injector. This was done by comparing the gas production by two producers with a scenario where one of the one is used for CO<sub>2</sub> injection.

The current geological model shows good connectivity between the B1 and the B5 producers. Injection in one of the 2 wells would possibly lead to rapid increases in the CO<sub>2</sub> concentration (breakthrough of the injected CO<sub>2</sub>) in the produced gas in the other. Maintaining both producers leads to the highest production.

#### P18-2.

The Road project is currently considering the injection of CO<sub>2</sub> into the depleted P18-4 compartment. This would involve the building of a pipeline for the transport of CO<sub>2</sub> from the Rotterdam area to this off-shore area. The off-shore access to CO<sub>2</sub> potentially opens the way for considering options for additional benefits. Examples would be a long-term pilot test in order to estimate the storage capacity of a virgin aquifer, without upfront investments, EOR and also EGR.

In 2012, the operator (TAQA) asked for the modelling of several EGR scenarios in the P18-2 compartment. This reservoir contains 3 producers. A history match (see feasibility report P18) concluded that the P18-2 compartment is in contact with an adjacent compartment, which also contains a producer. It appears, however, to be completely separated from the P18-4 compartment. The field has become mature, with current production forecasts predicting on-going production until 2017. At that time, the predicted reservoir pressure has dropped to 13 Bars. The maximum proposed injection rate was 1.1 Mton/year. The producer in the deepest part of the reservoir was converted into an injector, while the other producers maintained production, initially at production rates of 2017. A minimum Bottom Hole Pressure of 10 was applied in the simulations. To avoid contamination of the produced gas, a maximum concentration of 5% was requested by the operator. This was established by attaching monitors to the two remaining producers and to these close these wells, once the threshold has been reached. It should be noted that the ambient CO<sub>2</sub> in the reservoir is 1.2%, which means that only a limited elevation of the carbon-dioxide levels were allowed.

Initially, various injection rates were modelled, as well as different perforation configurations. All scenarios lead toward a higher ultimate recovery compared to a production stop in 2017. The initial results, however, were somewhat surprising as the ultimate recovery of the gas went up with reducing injection rates. This could be attributed to the high injection rates, the high permeability of the Hardegsen Fm and the very limited increase of CO<sub>2</sub>, which was allowed. The ultimate recovery did also not depend on using various perforation configurations did not have a significant impact on the ultimate recovery.

#### P18-4:

Increased injection rates were modelled for the P18-4 compartment. After a check, whether the current producer is capable of injecting between 2 and 3 T/year (possible as long as CO<sub>2</sub> is in dense phase) these injection rates were modelled.

## 4 CO<sub>2</sub>-EOR/EGR activities and results over 2012

This report provides an overview of the activities being made in the areas of carbonated water flooding and CO<sub>2</sub> storage in depleted oil fields, the general topic of PhD research.

This report provides an overview of the activities being made in the areas of carbonated water flooding and CO<sub>2</sub> storage in depleted oil fields, the general topic of PhD research.

During reporting period the following studies were undertaken:

### STUDY 1: STUDY ON SURFACE CHARGE AND SURFACE POTENTIAL (ongoing)

#### 1.1 THE STREAMING POTENTIAL EXPERIMENT

##### CHANGES IN THE EXPERIMENTAL APPROACH

The measurements are conducted with a use of laboratory set up that is shown in Figure 1A,B. The closed loop experiments have been change for an open system due to problems regarding closed circuits that could be created. The set up is almost ready for starting the experiments. A lot of problems regarding technical matter i.e. core preparation, conductivity sensor construction were encounter during reported period.

Further tests will be done in 2013. If results show reproducibility the experiment, then data together with analysis will be present in the next half year report. See results in Annex 1.

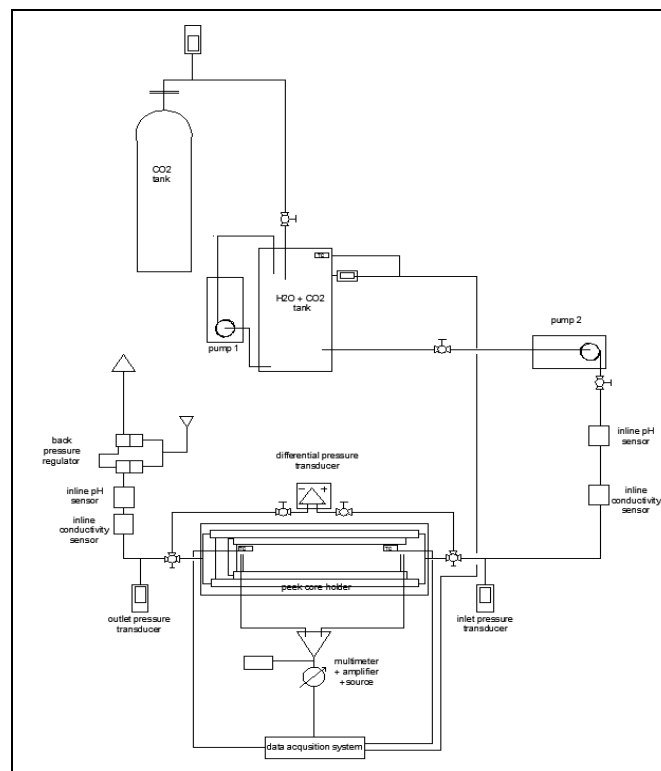
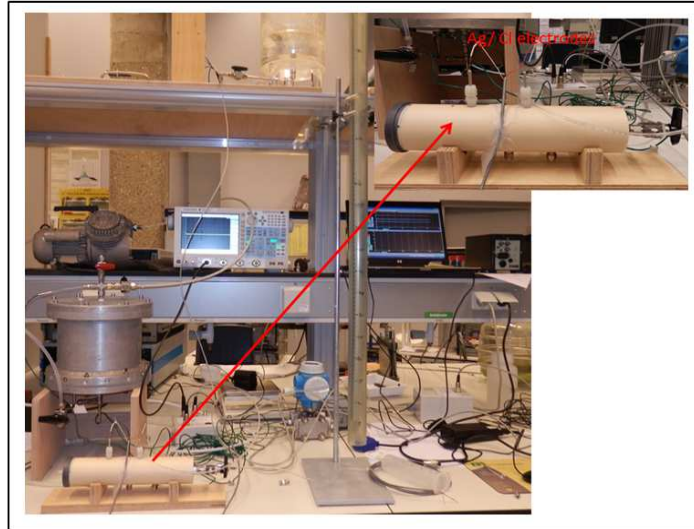


Figure 1A. Schematic description of the modified experimental set up.



**Figure 1B.** The experimental set up for study on surface charge and surface potential.

### 1.2 STATIC HEAD EXPERIMENT

Additional experiments were done with a use of Bentheimer sandstone and as well silica. Silica was used as a model sample to calibrate the system. The Bentheimer core and silica core ( $d = 3 \text{ cm}$ ,  $H_s = 3.6 \text{ cm}$ ) were prepare based on the same procedure as previous experiments (cores were placed in rubber sleeve and attached to a 1m long column  $H_w$ ). Two Ag/AgCl electrodes were placed in the core to measure streaming potential together with voltmeter and amplifier. The pressure difference was generated due to different water elevations above the sample. The pH and conductivity of the electrolyte were measured separately. The pore fluid conductivity  $\sigma_f$  was determined according to Archie's Law. The formation factor (F) was determined by calculations and the porosity measured experimentally  $\phi_B = 0.246$ ,  $\phi_s = 0.3$ ).

### RESULT ANALISYS

The results of measured streaming potential vs. fluid pressured difference and the calculated zeta potential vs. flow rate are presented in Fig.2 - 7. The achieved results (especially silica) are in line with the literature data. It means that the preliminary investigations of the used equipment and measurement method were successful.

#### BENTHEIMER

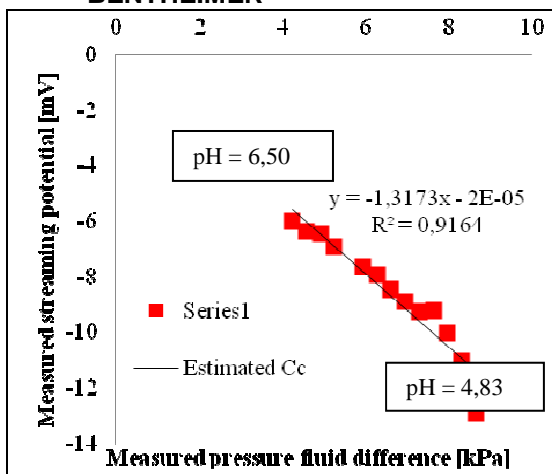


**Figure 2a.** Streaming potentials generated by pressure drops for the core test using the static head method

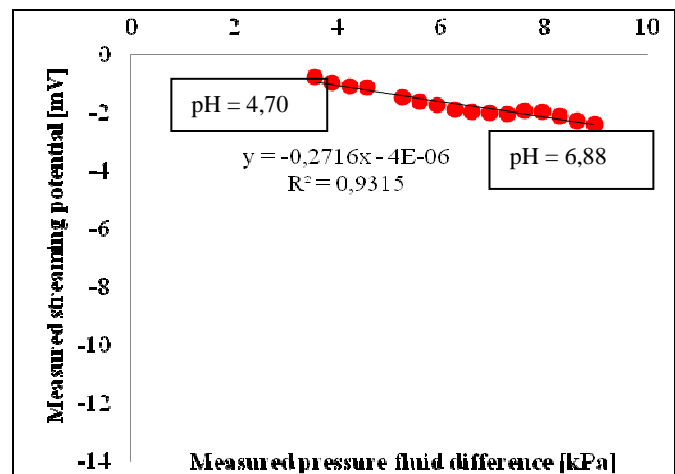


**Figure 2b.** Streaming potentials generated by pressure drops for the core test using the static head method

Investigation of the physical-chemistry of Carbonated Water Flooding

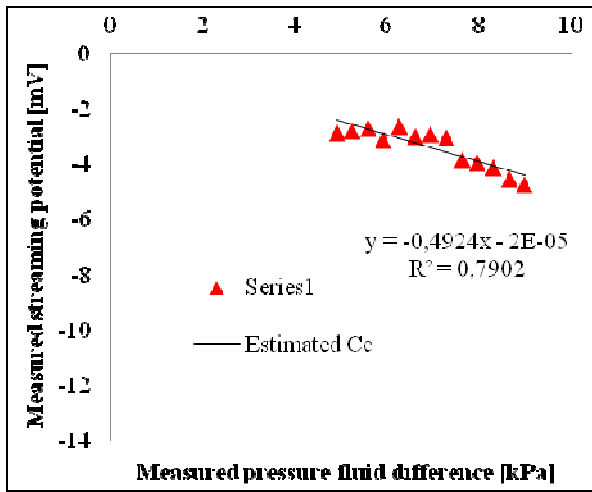


Figure 3. Streaming potentials generated by pressure drops for the core test using the static head method

SILICA

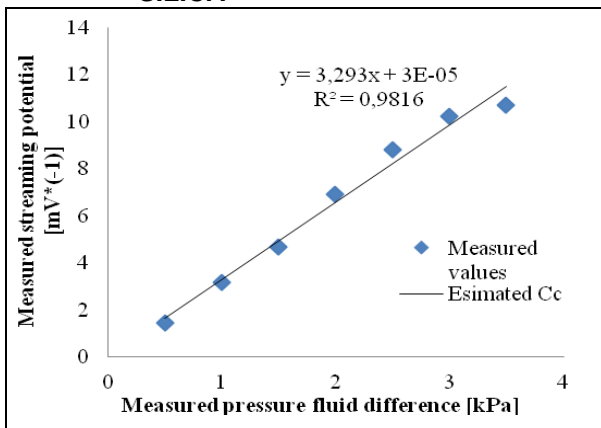


Figure 4. Streaming potentials generated by pressure drops for the core test using the static head method

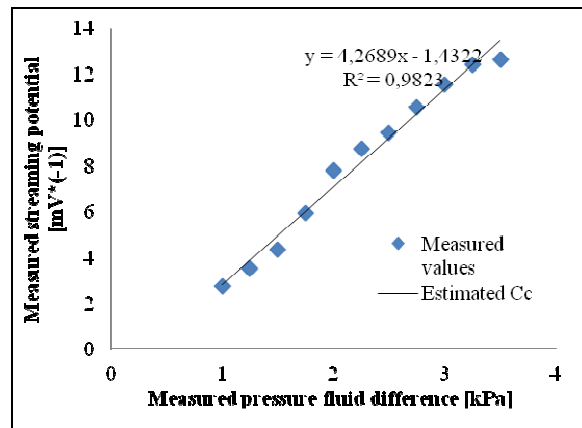


Figure 5. Streaming potentials generated by pressure drops for the core test using the static head method

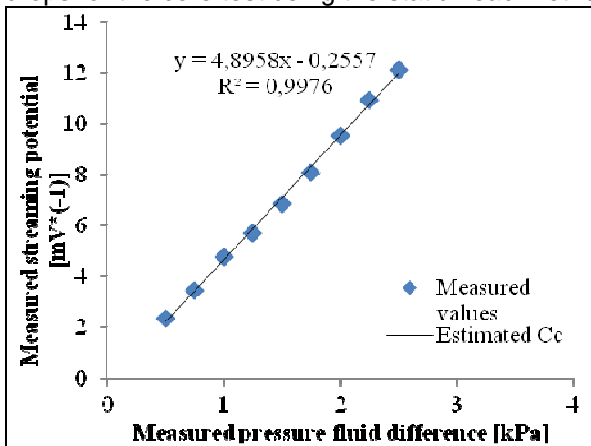


Figure 6. Streaming potentials generated by pressure drops for the core test using the static head method

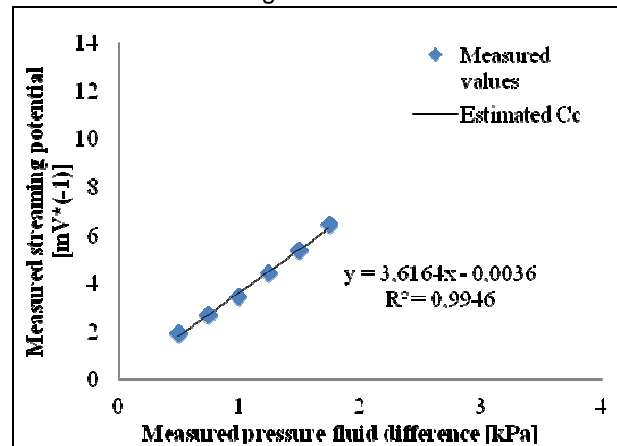


Figure 7. Streaming potentials generated by pressure drops for the core test using the static head method



### SPECIFIC SURFACE AREA

Very important parameter for the correct interpretation of the streaming potential experiment and potentiometric titration experiment is the specific surface area. The surface charge depends on it. The specific surface areas of Bentheimer sandstone and silica were obtained by different means:

- a consolidated Bentheimer sandstone and a consolidated silica were analyzed by a stereological estimation,
- a grained Bentheimer and quartz underwent a particle size and concentration analysis.

### POTENTIOMETRIC TITRATION

Adsorption on solids is strongly dependent on acid/base properties of the system, containing adsorbate and adsorbent. The pH changes may influence adsorption, ionic exchange and/or precipitation. The potentiometric titration is conducted for ascertaining the exact volume of titrant (0.1M HCl or 0.1M NaOH). It is chemically equivalent to a given amount of another substance, either blank electrolyte (H<sub>2</sub>O or brine) or a given amount of solid material (quartz or Bentheimer sandstone) dissolved in a electrolyte. The experiment provides possibility to estimate e.g. surface charge of quartz and Bentheimer by comparing the results of titration of different solid masses suspended in the solution against titration of the blank electrolyte (without solid). The influence of solid on the equilibrium can be established by use of the obtained difference of titrant quantity between respective points characterized by the same pH value. Observed differences can find explanation in an electric charge created on solid surface or dissolution of solid or as well both phenomena. Presence and influence of impurities is as well investigated. Moreover the dissolution constants are determined based on experimental results.

### EXPERIMENTAL APPROACH

The solution of a given amount of solid dissolved in electrolyte was stirred with a teflon magnetic stirrer for 24h before the experiment was started. The acid/base properties of mixtures were investigated before starting the main experiment. The pH values of different rock fractions showed that the Bentheimer sandstone increase the pH of the mixture (See Table 1).

The potentiometric titrations were performed in the nitrogen atmosphere (constantly stirred) by adding small equal amounts of HCl or NaOH to the solution cell. The pH data were recorded at certain time lapses (5min) after switching off the stirrer. During that time, the mixtures were continuously stirred, what allowed achieving the equilibration of the solution at particular stage of the experiment.

**Table 1.** The pH values of different rock fractions dissolved in the electrolyte (after 24h of stirring).

soild \ pH	pH (electrolyte: 100 ml of H <sub>2</sub> O)	pH (electrolyte: 100 ml of 2.2 mol/dm <sup>3</sup> NaCl solution)
No soild	5.6	
0,5 g Bentheimer	6.67	7.08
5g Bentheimer	8.62	8.87
10 g Bentheimer	9.10	9.35

### EQUIPMENT

The potentiometric titration was conducted by an apparatus that consists on: (1) 744 pH Meter; (2) high pressure nitrogen for removing CO<sub>2</sub> from the system; (3) automatic burette; (4) gas washing bottle with distilled water. A schematic representation of the set up and picture are presented in the figure 8 and 9.

## POTENTIOMETRIC TITRATION

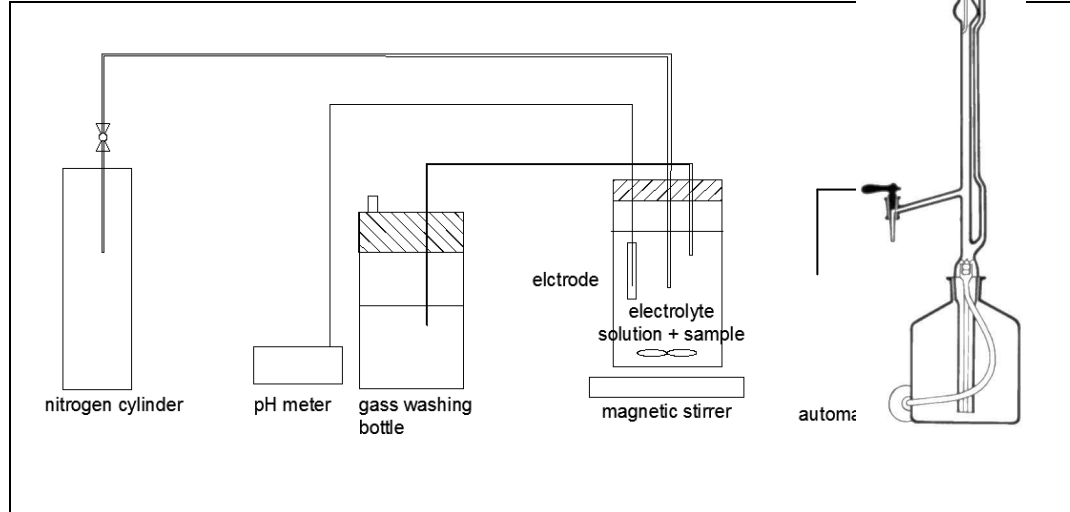


**Figure 8.** Schematic description of the potentiometric titration experimental set up.

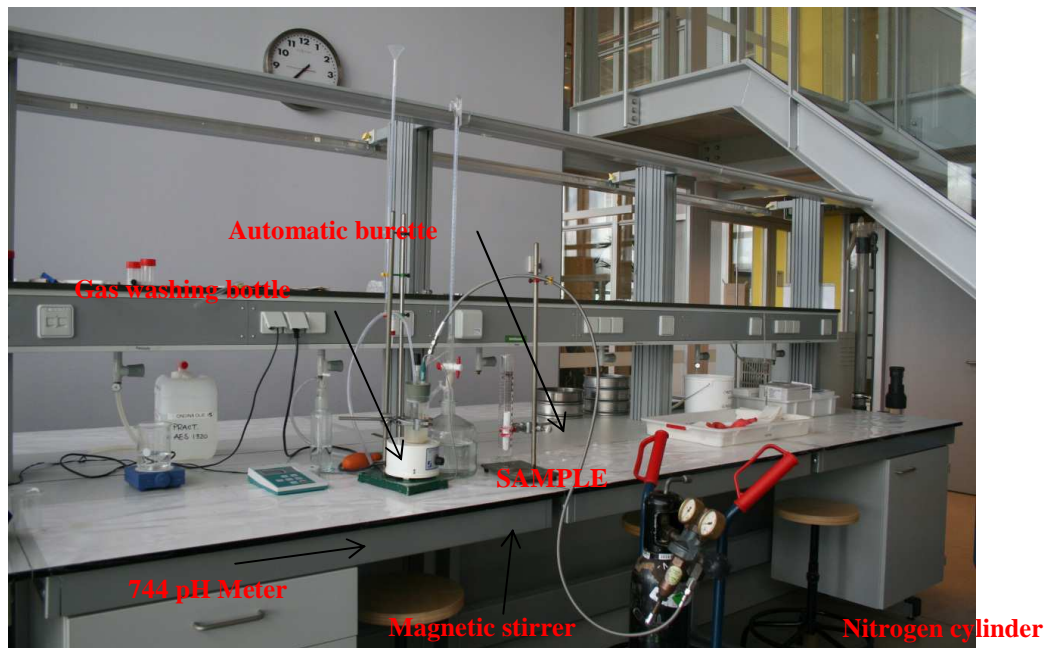


**Figure 9.** The potentiometric titration experimental set up.

## SAMPLES

Two different types of solids (only part of the obtained results is presented in the report) were chosen for potentiometric titration experiment: grained quartz and grained Bentheimer sandstone. Quartz samples were free of any impurities; the Bentheimer sandstone composition was mainly quartz (91.7 wt %), clays and feldspars (see Table 2 Annex 3).

Titration were performed for 3 different masses of solids (0.5g, 5.0g and 10g) in 75 and 100 ml of H<sub>2</sub>O (demineralized and degas), and in 75 and 100 ml of 2.2 mol/dm<sup>3</sup> NaCl solution (CATO brine). Additionally, titrations of blank electrolytes were performed for calculation purposes. The initial pH was established by addition of 8ml 0.1 mol/dm<sup>3</sup> NaOH. 0.1 mol/dm<sup>3</sup> HCl was used as a titrant.

**EXPERIMENTAL RESULTS** (examples of results)

**Acid/Base consumption curves**

The raw results of potentiometric titration are shown in figures 10 – 11 (Bentheimer sandstone) and in figures 12 -13 (quartz). The experimental data represent the consumption curves. They indicate that the acid consumption occurs due to creation of surface electric charge (adsorption of ions, dissociation of surface groups) and to the dissolution and/precipitation. The assumption is made that the electrolyte solution is saturated with dissolved sample.

Based on the raw results the point of zero charge and the differences in acid/base consumption balance can be obtained. Subsequently, data are used to calculate surface charge and acid/base consumption for sample dissolution.

The points of the mass titration curves intersections (Figure 10 – 13) are called CIP (common intersection point). In the case of figure 11, CIP lies as well on blank electrolyte titration curve, then can be called a point of zero charge (PZC). If CIP lies near to electrolyte titration curve (figure 10) it indicate that the additional aspects like: solid dissolution or occurrence of impurities need to be considered in this pH range when surface charge is computed. The  $pH_{pzc}$  values obtained from experiments are 8.5 for Bentheimer sandstone and 2.3 for quartz.

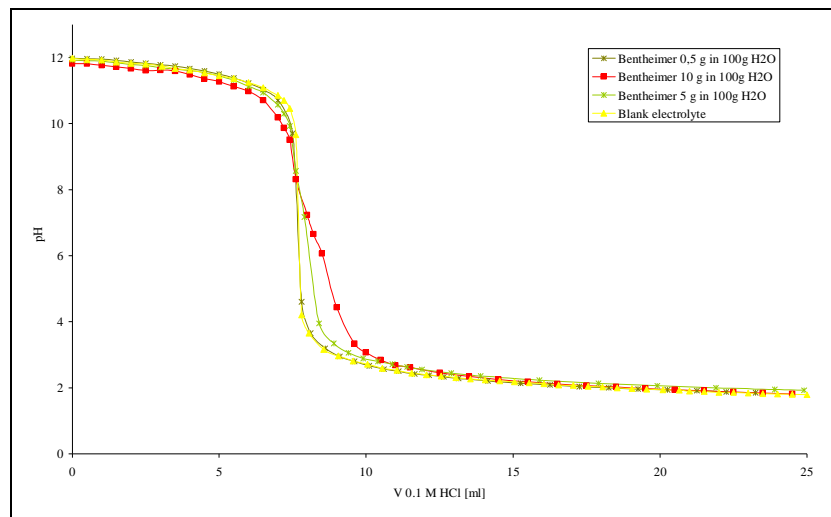


**Figure 10.** Potentiometric titration of Bentheimer sandstone dissolved in water (sample 1a – 1c) (Experimental conditions  $T = 22\text{ }^{\circ}\text{C}$ )

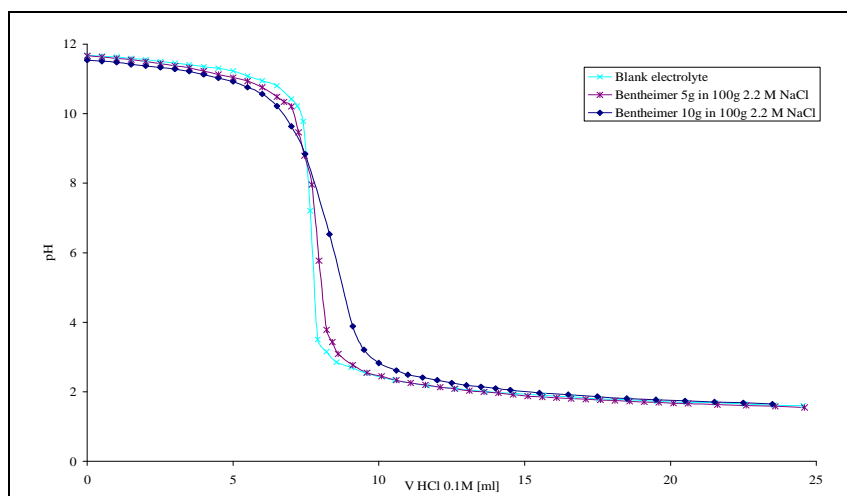


**Figure 11.** Potentiometric titration of Bentheimer sandstone dissolved in brine (sample 2a – 2b) (Experimental conditions  $T = 22\text{ }^{\circ}\text{C}$ )

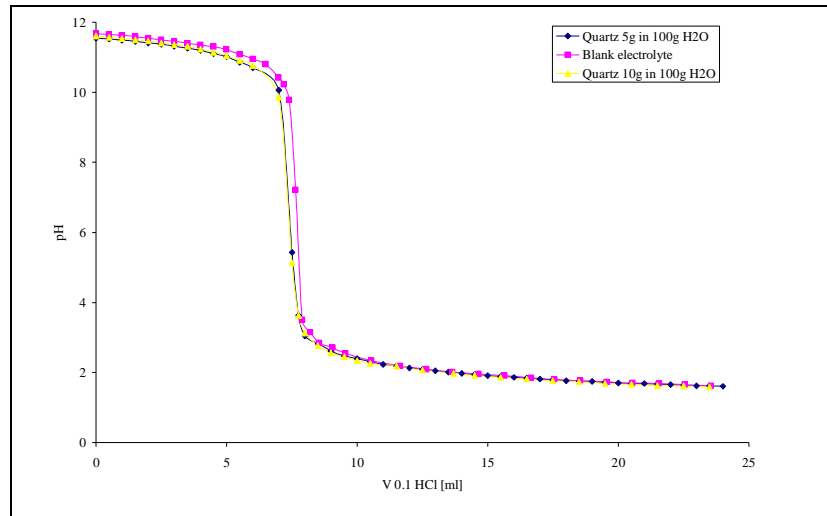


**Figure 12.** Potentiometric titration of quartz dissolved in water (sample 3a – 3b)  
 (Experimental conditions  $T = 22\text{ }^{\circ}\text{C}$ )

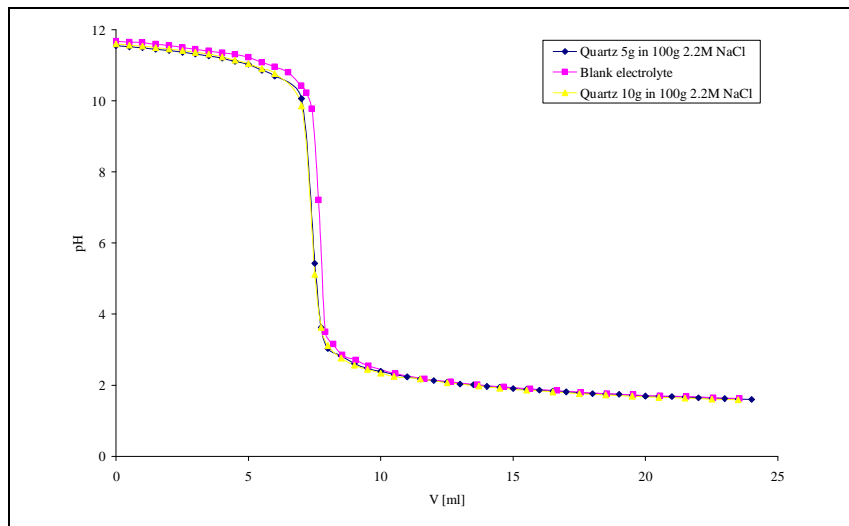


**Figure 13.** Potentiometric titration of quartz dissolved in brine (sample 3a – 3b)  
 (Experimental conditions  $T = 22\text{ }^{\circ}\text{C}$ )

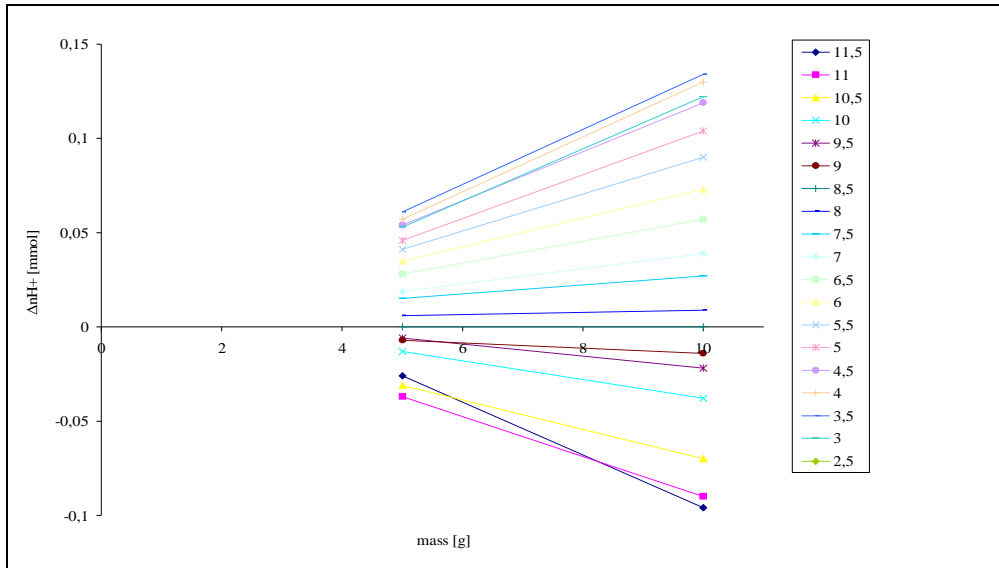


**Figure 14.** The proton balance for 5g and 10g of Bentheimer solution. Extrapolations of the lines and their y-intercept correspond to solid dissolution.

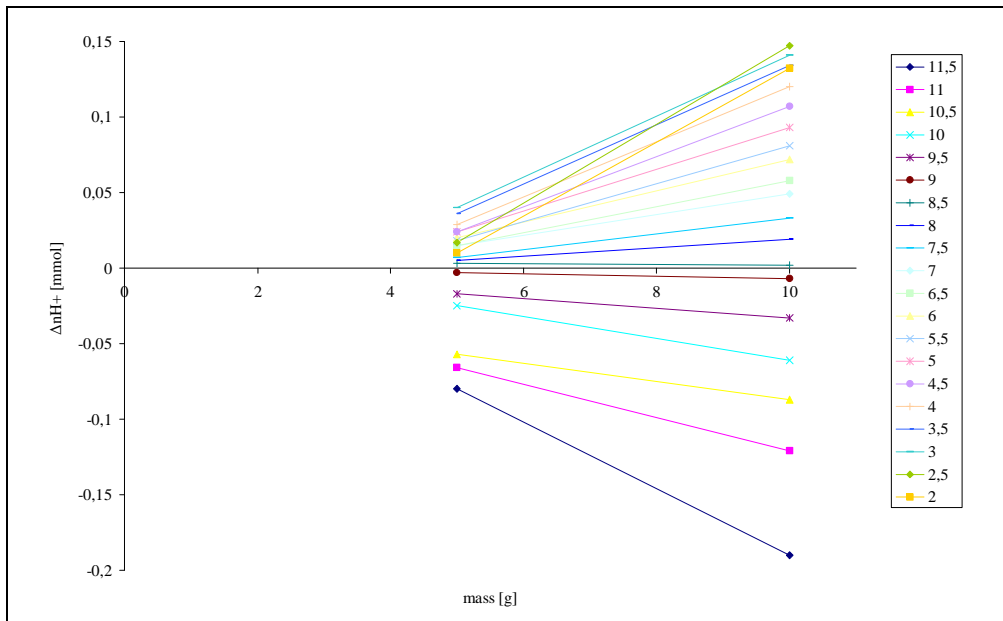


**Figure 15.** Proton balance for titration of Bentheimer in NaCl solution

#### Proton balance for titration of Bentheimer solution

The figures provides information about the actual values of  $\Delta n_{H^+}$  for two masses 5g and 10g of Bentheimer sandstone in 100 ml of  $H_2O$  electrolyte (see figure 14 Annex 3) and in 100 ml of  $2.2 \text{ mol/dm}^3$  NaCl electrolyte solution (see figure 15 Annex 3). The values are calculated from raw data at certain fixed pH (every 0.5 pH). The extrapolation of the lines up to point of zero mass (Y-intercept) gives the balance of protons (positive - protons are donated by the solid, negative – protons are accept). It is related to the overall effect of dissolution and impurities on pH.

#### Surface charge and dissolution effect

The surface charge,  $q_s$  was calculated with following equation:

$$q_s(pH) = - \frac{F \cdot (\Delta n_{sol, H^+}(pH) - \Delta n_o)}{ma_s}$$

The obtained results together with proton balance related to the dissolution effects are presented in figures 16 and 17.

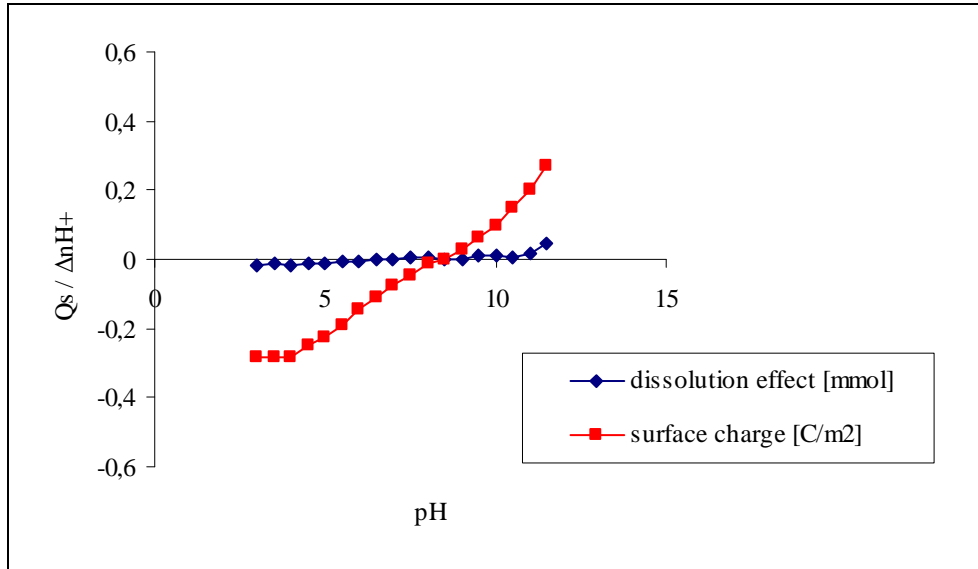


Figure 16. Surface charge density  $Q_s$  and sample dissolution effect for Bentheimer in  $H_2O$

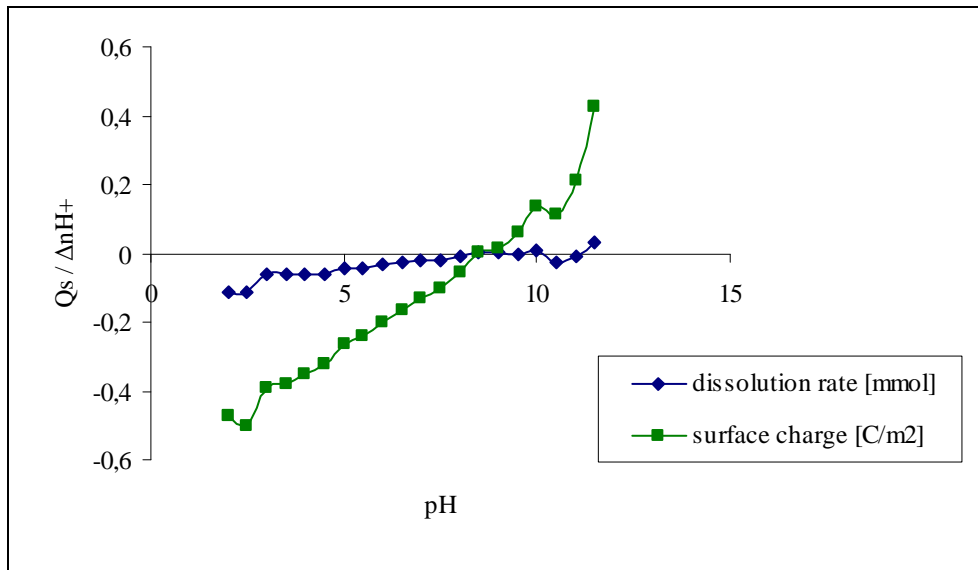


Figure 17. Surface charge density  $Q_s$  and sample dissolution effect for Bentheimer in NaCl solution.

### STUDY 2-Part 1: STUDY ON MOLECULAR DIFFUSION OF CO<sub>2</sub> FROM CARBONATED WATER (CW) INTO THE OIL (ongoing)

The goal of this study is to determine the effect of CO<sub>2</sub> diffusion from CW into oil. The “binary” system CO<sub>2</sub>-oil / CO<sub>2</sub>-water is considered as promising option with favorable phase behavior effects, where carbonated water (CW) is in direct contact with the oil. However, by this date, the precise determination of the role of diffusion has not been quantified and the literature data are limited. For

investigating the CO<sub>2</sub> diffusion from CW into oil as a function of time, oil swelling factor and determination of the distribution of the total dissolved CO<sub>2</sub> (partition coefficient) between the coexisting phases: water (brine) and oil phase the micromodel will be build. The experiment is at the level of preparation. Set up shown in Figure 1 is under construction. The preliminary studies and measurements of the possible options of improving designed set up have been conducted.

### BACKGROUND OF THE STUDY

Molecular diffusion of CO<sub>2</sub> from carbonated water into oil is an important process in mobilization and recovery of residual oil in water wet rock and in the CO<sub>2</sub> storage. It influences oil viscosity, and as a result, swelling. A lot of studies regarding diffusion of carbon dioxide in CO<sub>2</sub> flooding have been undertaken (Grogan and Pinczewski, 1987; Campell et al., 1985; McGuire and Stalkup 1992; Bijeljic et al., 2002). In spite of many undertaken investigations, the time and scale of diffusion process are still not exactly specified.

The diffusion from CW into the oil occurs due to much higher solubility of carbon dioxide in both water and oil compared to water in oil and hydrocarbons in water. This process is time depended (CO<sub>2</sub> concentration increase with time at the interface between two phases (oil- CO<sub>2</sub>/CO<sub>2</sub> -water), and phase composition depended. Nonetheless, there is no available data on physical properties for oil/water/ CO<sub>2</sub>, and therefore most of the authors assume models where lack of dependence on phase composition exists (Grogan and Pinczewski, 1987). Sohrabi et al. (2011) created model based on the flow visualization experiments with a use of high pressure, transparent micromodels. They obtained the quantitative and qualitative data, that enable them to create one – dimensional, mathematical model. Thought, the results are not reliable, because of the value of partition coefficient used by them.

### EXPERIMENTAL APPROACH

The CW - oil 1-D diffusion experiment will be conducted with use of experimental set up presents in the figure 18. This idea has been chosen to minimize effects of gravity segregation. The experimental set up consists on: consist of a micromodel, aluminum cell holder, fluids sources, syringe pumps, pressure transducer, a timer, a video camera and valves. A horizontal transparent capillary/slim glass tube (3-5mm in diameter) is placed in the cell holder with a window in front of the tube.

### MOLECULAR DIFFUSION OF CO<sub>2</sub> FROM CARBONATED WATER INTO THE OIL

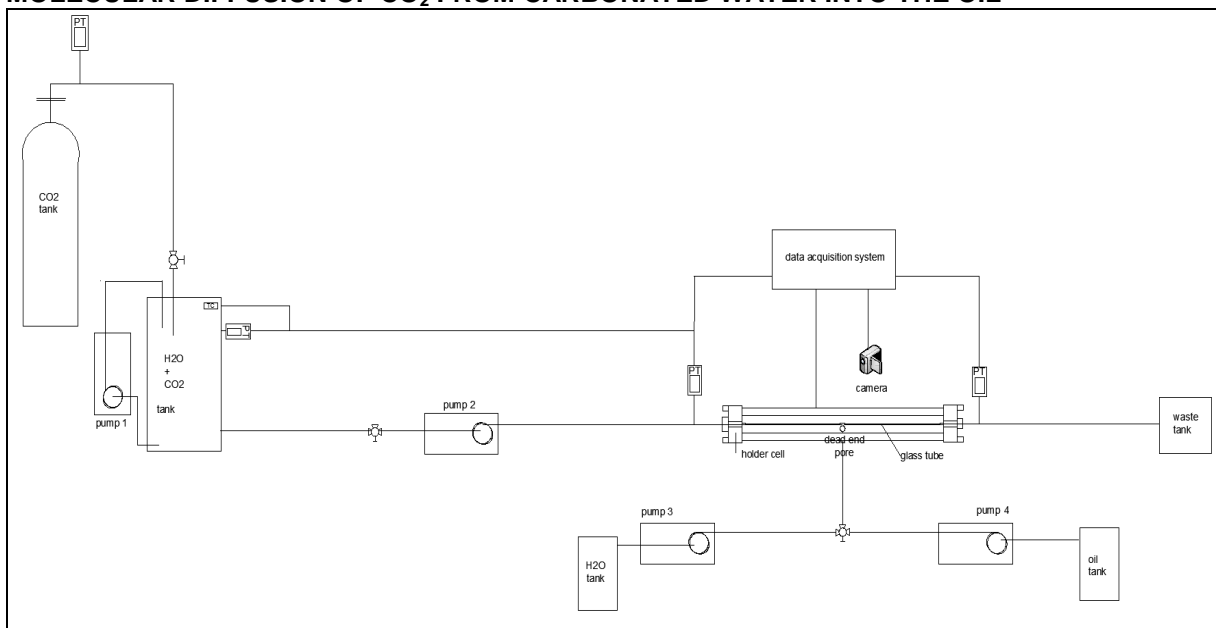


**Figure 18.** Schematic description of the experimental set up.



## **STUDY 2-Part 2: STUDY ON MOLECULAR DIFFUSION OF CO<sub>2</sub> FROM CARBONATED WATER (CW) INTO THE OIL**

(One of the important CWF processes is molecular diffusion of CO<sub>2</sub> from carbonated water into oil (DCWO). The process benefits from oil viscosity reduction, an increase in oil relative permeability and as a result enhancement of oil mobility. In order to get the distribution (partition coefficient) of the total dissolved CO<sub>2</sub> between the coexisting phases, brine and oil, we examine DCWO in experiments with respect to oil swelling factor over time. In contrast to many previous studies on diffusion of carbon dioxide in CO<sub>2</sub> flooding, DCWO characterization is underexposed in laboratory work and literature. The results of the conducted experiment can contribute to a better understanding of molecular diffusion in CWF. In addition, DCWO results lead to process improvements for achieving recovery in both laboratory core floods and in the field with an option for CO<sub>2</sub> sequestration.

Based on preliminary results we expect a dominant role of diffusion in the CW recovery and existence of ample contact time to recover oil sufficiently

### **CHANGES IN THE EXPERIMENTAL APPROACH**

To determine the phase behaviour of the system 1-D pore-scale diffusion experiments are conducted (see figure 18). In order to satisfy all measurement and safety requirements we have modified the setup. The aluminium core holder with a glass tube has been changed to a set of five PEEK connectors (3 tees and 2 crosses) that mimic dead end pores. All of the connectors are linked to each other by a PEEK tubing. Each tee connector hosts a thermocouple, and a cross connector hosts a thermocouple and an electrode for conductivity measurements. PEEK has been chosen due to its high temperature and pressure resistance. CO<sub>2</sub> – rich brine is stored and mixed in the transfer vessel to keep the pressure and CO<sub>2</sub> solubility at a constant level. Pressure transducers are installed before and after the set of connectors to determine the pressure drop that is related to oil CO<sub>2</sub> sorption.

### **EXPERIMENTAL PROCEDURE**

The experimental procedure consists of: (1) saturating the system (tubing + connectors) with oil; (2) displacing oil by waterflooding until water breakthrough (residual oil will be located in dead end pores); (3) carbonated water flooding with a rate of 1ml/h. CT scanning of the entire process is performed. In these experiments oil, initially placed in a dead-end pore, swells due to CO<sub>2</sub> diffusion from a CW stream under PT-conditions. As a result, after some time, pressure and oil-composition dependent, recovery of oil occurs.

### **EXPERIMENTAL MATERIALS**

#### **OIL:**

Hexadecane: API (52), SG (0.773), MW (226.446 g/mol)

Crude oil: API (26.4), SG (0.895), MW (385 g/mol)

#### **BRINE:**

CATO2 brine: 130 g/L NaCl, 8 g/L Ca<sup>++</sup> (≈ 22.2 g/L CaCl<sub>2</sub>), 1 g/L Mg<sup>++</sup> (≈ 4 g/L MgCl<sub>2</sub>)

### **DIFFUSION MODEL**

The laboratory results are used to build an enhanced diffusion model for oil, CO<sub>2</sub> - H<sub>2</sub>O.

## **Study 2 part3: STUDY ON CO<sub>2</sub> SORPTION CAPACITY OF OIL**

Direct contact between oil and gas is often observed in a petroleum reservoir and in many unit process operations, where the solubility of gases in liquids has an important role in the description of the phase behaviour of these systems. In the case of my research sorption capacity of oil plays an important role in all conducted experiments, especially in DCWO. Though the determination of the CO<sub>2</sub> sorption capacity of crude oil in reservoir conditions (elevated temperature and pressure) is essential.



Certainly, there is large amount of correlations available in the literature, valid for wide range of API°, but data obtain directly for certain PT condition and composition are more accurate.

### EXPERIMENTAL SETUP

The main objective of the study is to measure the carbon dioxide pressure drop and oil swelling due to the dissolution process. For this purpose suitable laboratory setup that can be charged with different initial pressures of CO<sub>2</sub> and subsequently disconnected from surroundings, were constructed. A laboratory set up consists on two separate parts that operates in the same time (see figure 19 and 20): (1) Stainless steel vessel ( $V_1 = 160\text{cm}^3$ ) and (2) Vessel made of glass, placed in the aluminium core holder ( $V_2= 25\text{ cm}^3$ ).

### EXPERIMENTAL PROCEDURE

Procedure for both of the parts of the setups operation is exactly the same. A known amount of oil is placed in a stainless steel sample cell ( $V_o = 32\text{ml}$ ) and in the glass tube ( $V_o = 5\text{ml}$ ). Subsequently a known amount of carbon dioxide is added to the vessel and to the glass tube. CO<sub>2</sub> is introduced into the reactors from a high pressure cylinder with use of pump. Both parts are held in the thermal systems (glass tube in the water bath and vessel in the oven) to obtain reservoir conditions. Additionally, glass tube with window, allows to monitor swelling process of the oil. By mass balance, the moles of CO<sub>2</sub> adsorbed by the liquid phase or phases is then determined.

The decane is used as a model oil to validate the equipment, because the data sets and correlations are available in the literature for this hydrocarbon. The main experiment is conducted on crude oil, the one that is used in all other experiments of CWF research.

There were 4 sets of experiments (4x5 injection rates) conducted with use of decane to prove reproducibility and 2 sets of experiments with crude oil. The experiments are still on-going.

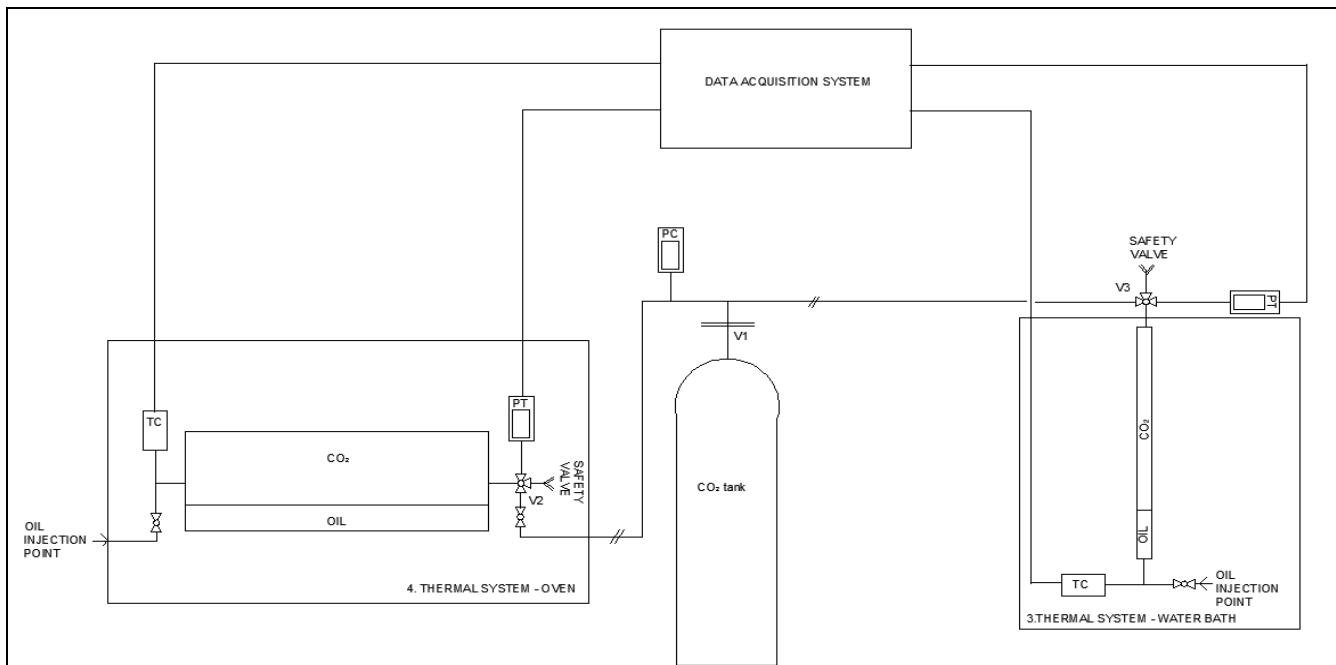


**Figure 19.** Schematic description of the experimental set up for CO<sub>2</sub> sorption experiments.



**Figure 20.** The experimental set up for CO<sub>2</sub> sorption experiments.

## EXPERIMENTAL MATERIALS

### OIL:

Decane: API (62.5), SG (0.73), MW (142.280 g/mol)  
Crude oil: API (26.4), SG (0.895), MW (385 g/mol)

### GAS:

The model gas – CO<sub>2</sub> (4.5 K55OH UN1013 produced by Lindau). The composition of the gas is given by CO<sub>2</sub> ≥ 99.995 vol%, N<sub>2</sub> ≤ 30 vpm, O<sub>2</sub> ≤ 15 vpm, H<sub>2</sub>O ≤ 5 vpm, C<sub>x</sub>H<sub>x</sub> ≤ 2 vpm.

## EXPERIMENTAL RESULTS

The solubility of carbon dioxide contributes to changes in the oil physical properties. Some of them are affected in larger extent (viscosity, swelling) than others i.e. density less. The scale of influence may depend on different factors, inter alia oil composition, pressure, temperature. Among above the composition is very significant, because crude oil can contain many different components, that determine its physical properties.

### - CO<sub>2</sub> SORPTION CAPACITY OF OIL

The results of experiments with use of decane are compared with available data and commonly known correlations (f.ex. Emera and Sarama, 2006). It shows that the setups are working properly and can be used for determination CO<sub>2</sub> sorption capacity of crude oil (Figure 20).

Based on the conducted experiments we can conclude:

- The solubility of carbon dioxide in the glass tube is much slower than in the vessel. It is due to: (1) increasing solubility of CO<sub>2</sub> in the oil by shaking the reactor; (2) much larger interfacial area CO<sub>2</sub>/oil (glass reactor is placed vertically; stainless steel vessel is placed horizontally). The time required for achieving equilibrium state for a glass tube is around 5-7 days, and for stainless steel vessel less than 1 hour.
- Obtained values of solubility are very similar to existing data, although for higher pressures (>60 bar) they are larger. It can be a result of lack of appropriate SF value for higher pressures.
- figures 21, 22 show comparison of pressure drop for decane and crude oil. It can be deduced that with this kind of reactor, equilibrium may be achieved in very short time scale (< 1 hour).

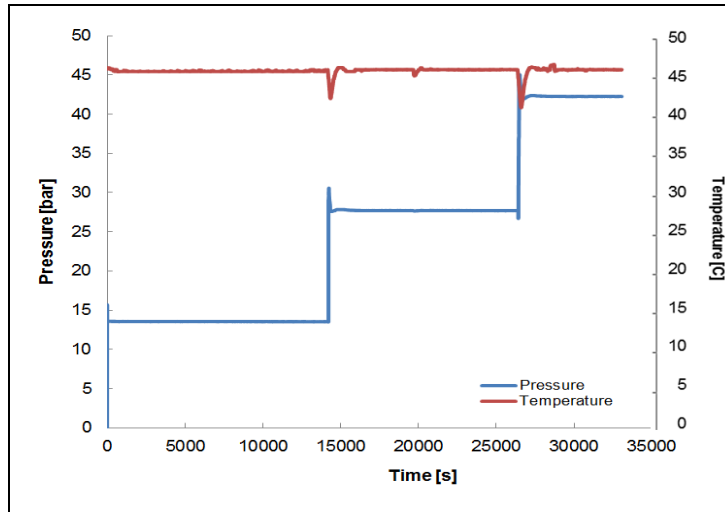


**Figure 21.** Pressure vs. time and temperature vs. time during sorption experiment 3 in the stainless steel vessel (example). The initial mass of decane was 20g (1/5 volume of the vessel), and an initial pressures of particular steps 15.5, 31 and 45 bar.

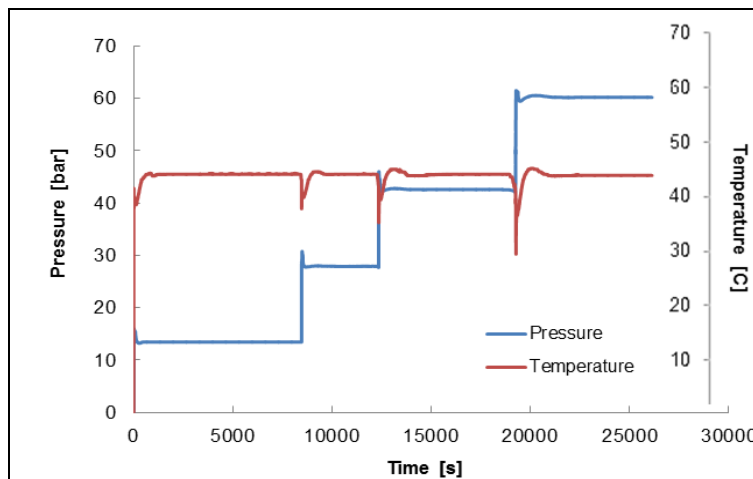


**Figure 22.** Pressure vs. time and temperature vs. time during sorption experiment 7. The initial mass of crude oil was (1/5 volume of the vessel), and an initial pressures of particular steps 15.5, 30, 45 and 60 bar.

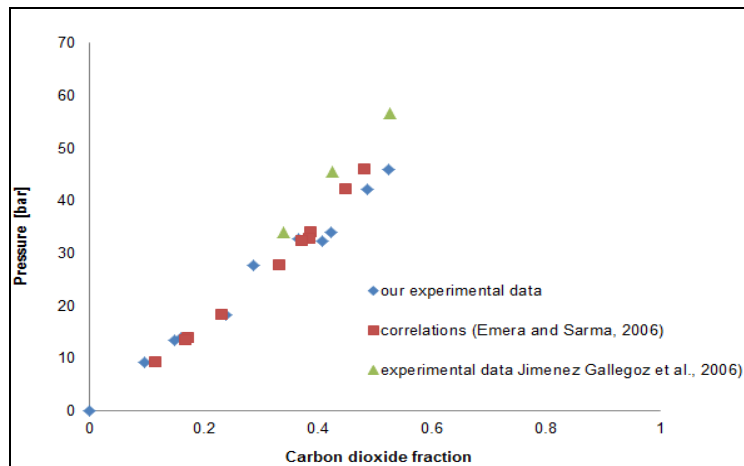


**Figure 23.** Pressure composition graph. It represents comparison of results obtained in our experiment and data available in literature.

**- SWELLING FACTOR (SF)**

Process of carbon dioxide dissolution in the oil causes an increment in the oil formation volume factor. In other words the apparent volume of the oil in place is enlarged. Based on the experimental observations of volume change (glass tube experiment) the swelling factor of decane and crude oil is determined (Figure 24). The oil swelling factor is a ratio of CO<sub>2</sub>-saturated oil volume at the reservoir conditions (pressure, temperature) to the oil volume at the same temperature and pressure equal to the oil bubble point pressure (P<sub>b</sub>) (Emera and Sarma, 2006). The results of study on decane show that the results are a bit smaller than the correlation, but in the same range. Correlations are used with assumption that oil swelling is directly related to CO<sub>2</sub> solubility. It brings the conclusion that the experimental set up may be used for determination of SF of crude oil. Experiments are currently on-going, therefore data will be provided in the next report.

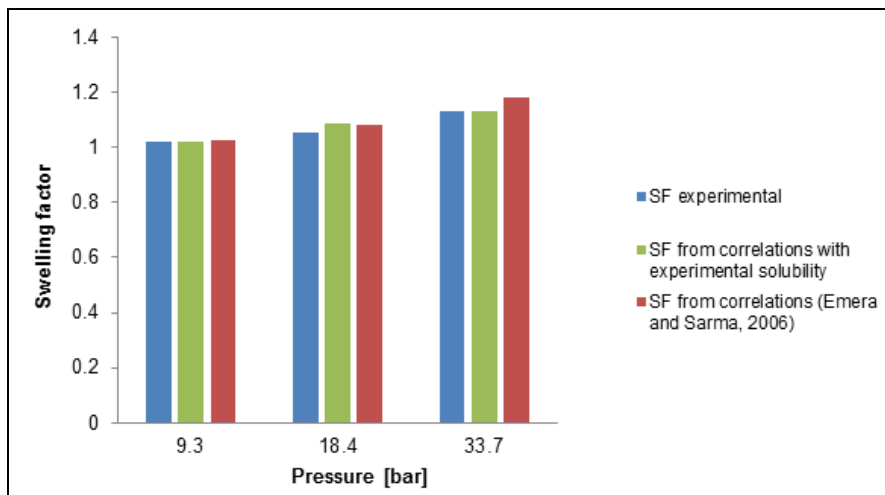


**Figure 24.** Swelling factor vs. pressure (comparison of obtained data with data from correlations (Emera and Sarma, 2006 (both for correlated solubility and solubility from experiments)).

**STUDY 3: PETROGRAPHICAL AND PETROPHYSICAL PROPERTIES OF BENTHEIMER SANDSTONE**

The specific resistivity model of the Bentheimer sandstone is under construction. It is based on the mineral composition data obtained from XRD and XRF analysis (see Table 2) and literature data regarding the specific resistivity of particular minerals. The main goal is to determine influence of clays on electro-kinetic properties of Bentheimer. The specific resistivity model of the Bentheimer sandstone is under construction. The new images of Bentheimer were obtained. The images were done on the thin section but without glass plate on the top to avoid reflection effect. Grain size analyses on new images were done. Additionally CT scans of pencil Bentheimer were prepared to create 3D model of the sandstone. The experimental set up is ready and preliminary tests were done (see Figure 1b).

**Table 2.** Composition data of Bentheimer sandstone obtained from XRF and XRD.

MINERAL			Ours			
			Quarry Romberg			
			mole %	wt %	vol %	
Silicate minerals	Clay	QUARTZ	97,78	91,70	91,62	
		ILLITE	-	-	-	
		KAOLINITE	0,62	2,50	2,55	
		MONTMORILLONITE	0,03	0,18	0,18	
		CHLORITE	-	-	-	
	Mica		MUSCOVITE	-	-	-
	Feldspar	Plagioclaste	ALBITE (Na)	-	-	-
			ORTHOCLASE	1,12	4,86	5,03
	Alkali	MICROCLINE	-	-	-	
Carbonate mineral	SIDERITE		-	-	-	
	DOLOMITE		0,18	0,26	0,24	
	CALCITE		0,09	0,15	0,14	
	MAGNESITE		-	-	-	
Oxide mineral	HEMATITE		0,06	0,16	0,08	
	GIBBSITE		-	-	-	
	GOETHITE		-	-	-	
	RUTILE		0,06	0,03	0,04	
	ANATASE		-	-	-	
Fe Sulfide mineral		PYRITE	0,01	0,01	0,01	
Sulfate mineral		GYPSUM / ANHYDRITE	-	-	-	
		CA-PHOSPHATE	0,01	0,07	0,06	
		HALITE (NaCl)	0,04	0,03	0,04	
		ORGANIC MATTER	-	-	-	
		FREE WATER	-	-	-	
<b>SUM</b>			100,00	99,96	100,00	